Energy & Environmental Science

Accepted Manuscript

Organic Photovoltaic Greenhouses: A Unique Application for Semi-transparent PV?†

Christopher J M Emmott,[*a,b,‡] **Jason A Röhr,**[a,c,‡] **Mariano Campoy-Quiles,**[d] **Thomas Kirchartz,**[e,f] **Antonio Urbina,**[a,g] **Nicholas J Ekins-Daukes,**[a] **and Jenny Nelson**[a,b]

Received Xth XXXXXXXXXX 20XX, Accepted Xth XXXXXXXXX 20XX
First published on the web Xth XXXXXXXXXX 200X
DOI: 10.1039/b000000x

Organic photovoltaics is an emerging solar power technology which embodies properties such as transparency, flexibility, and rapid, roll to roll manufacture, opening the potential for unique niche applications. We report a detailed techno-economic analysis of one such application, namely the photovoltaic greenhouse, and discuss whether the unique properties of the technology can provide advantages over conventional photovoltaics. The potential for spectral selectivity through the choice of OPV materials is evaluated for the case of a photovoltaic greenhouse. The action spectrum of typical greenhouse crops is used to determine the impact on crop growth of blocking different spectral ranges from the crops. Transfer matrix optical modelling is used to assess the efficiency and spectrally resolved transparency of a variety of commercially available semi-conducting polymer materials, in addition to a non-commercial low-band-gap material with absorption outside that required for crop growth. Economic analysis suggests there could be a huge potential for OPV greenhouses if aggressive cost targets can be met. Technical analysis shows that semi-transparent OPV devices may struggle to perform better than opaque crystalline silicon with partial coverage, however, OPV devices using the low-band-gap material PMDPP3T, as well as a high efficiency mid-band-gap polymer PCDTBT, can demonstrate improved performance in comparison to opaque, flexible thin-film modules such as CIGS. These results stress the importance of developing new, highly transparent electrode and interlayer materials, along with high efficiency active layers, if the full potential of this application is going to be realised.

1 Introduction

Solar Photovoltaics (PV) offer the potential for large scale low carbon electricity generation. However, large areas of land may be required for PV to meet rising energy demands. Therefore, innovations in developing multiple uses for the solar energy incident on a given area are required. Agrivoltaics denotes a system designed to combine commercial agriculture and photovoltaic electricity production within the same land area.[1] This idea is becoming increasingly prominent as densely populated regions of the world face increasing deployment of solar power.[2] One approach to agrivoltaics is the photovoltaic greenhouse where part of the solar radiation that is incident on a greenhouse roof is harvested by PV modules.

The PV greenhouse concept has been previously implemented through a variety of approaches as shown in figure 1. The partial shading approach (figure 1a) has been applied with both crystalline silicon and thin-film PV modules[3–8] where it has been found that with optimum spacing, coverage of 20-30% of the roof with PV does not impact crop growth.[5,9] A variant of this first approach has been to utilise only direct insolation for photovoltaic generation, whilst allowing diffuse light to penetrate the greenhouse, through the use of a Fresnel lens (figure 1b).[10,11] Such systems have been shown to be effective at allowing crop growth in addition to substantial electricity generation but require expensive and sophisticated tracking equipment.

The third approach has implemented semi-transparent PV modules (figure 1c)[12–14] or partially reflective coatings on the greenhouse glass which reflect light onto opaque modules.[15] This approach can allow maximum usage of the photosynthetically relevant light to reach the plants, whilst harnessing unused wavelengths for electricity generation. However, it is limited by the inflexibility in tuning the absorption spectra of

† Electronic Supplementary Information (ESI) available: Plots showing the refractive indices and extinction coefficients used in the optical modelling of all materials studied can be found in the ESI . See DOI: 10.1039/b000000x/
‡ These authors contributed equally to this work.

[a] *Department of Physics, Imperial College London, London SW7 2AZ, Tel: 02075947627; E-mail: christopher.emmott@imperial.ac.uk*
[b] *Grantham Institute for Climate Change, Imperial College London, London SW7 2AZ, UK.*
[c] *Department of Chemistry, Imperial College London, London SW7 2AZ, UK.*
[d] *Institut de Ciència de Materials de Barcelona (ICMAB-CSIC), Campus UAB, Bellaterra, 08193, Spain*
[e] *IEK 5 Photovoltaik, Forschungzentrum Jülich, 52425 Jülich, Germany.*
[f] *Faculty of Engineering and CENIDE, University of Duisburg-Essen, Carl-Benz-Str. 199, 47057 Duisburg, Germany.*
[g] *Departamento de Electrónica, Tecnología de Computadoras y Proyectos, Universidad Politécnica de Cartagena, Murcia, Spain.*

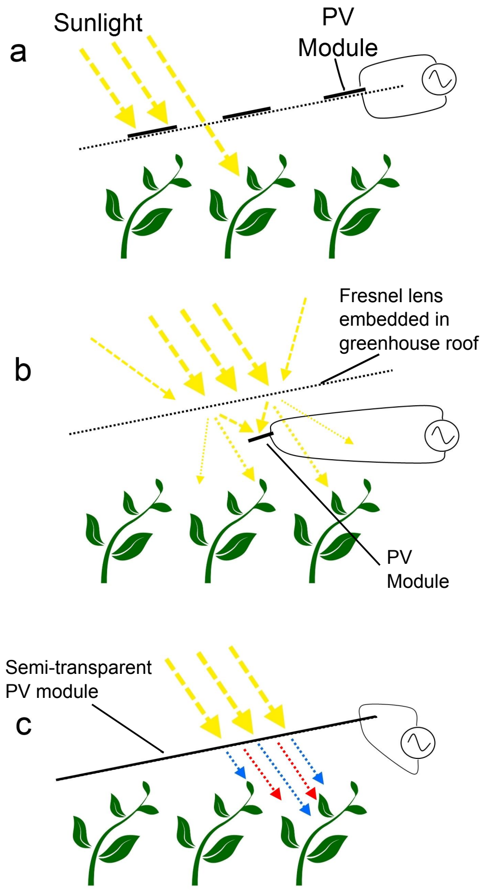

Fig. 1 Schematics of the various approaches to PV greenhouses. (a) Partial shading with opaque cells or modules; (b) focusing of direct light; (c) semi-transparent PV modules.

semi-transparent PV modules.

A solution is offered by solar cells based on molecular semiconductors. Organic photovoltaic (OPV) materials provide finite bandwidth absorption which, through manipulation of the molecular structure, can be tuned to absorb light not required for crop growth. This solution processable technology also allows for rapid large scale manufacture, offering the potential for very low costs and rapid carbon emission mitigation.[16–18] Plastic, largely low density polyethylene, is the dominant material used in greenhouse structures, known as polytunnels, and is very similar to substrate materials used in OPV, making this technology very compatible with this application. Semi-transparent OPV modules are being actively developed for building integrated applications[19–21], however, there has been minimal consideration of the use of the technology in a greenhouse application.[12,14,22] Here we evaluate this niche application of OPV.

1.1 Scope

Until now, the optical properties of OPV have only been explored within window applications where partial transmission in the visible spectrum is required.[20,23] No attempt has yet been made to optimise spectral absorbance to enable plant growth. In this paper, we assess the potential for OPV technology to be used effectively within a photovoltaic greenhouse. This analysis demonstrates a methodology for developing design rules and technology development aims towards a specific application.

We present a model of the PV generation and impact on crop growth of semi-transparent OPV used in greenhouse structures as a function of material choices and device designs. We evaluate currently available and widely studied polymers, which have the potential for scalable manufacture[24], as well as a promising low band gap polymer currently used in tandem devices, which allows for high transmission of light in the visible region. We discuss the limits to the performance of OPV greenhouses. On the basis of these analyses, the economics of an OPV greenhouses are considered as well as their global potential, and the technology is compared with other PV technologies which could be used in PV greenhouses.

2 Methods

2.1 Modelling crop growth

The different regions of the solar spectrum have a variety of effects on a greenhouse, as shown in figure 2. The visible region of the spectrum is often known within horticulture as photosynthetically active radiation (PAR). Photosynthesis utilises light within the bandwidth of around 400 nm to 700 nm, however, not all wavelengths are utilised to the same efficiency, with two peaks in the rate of photosynthesis occurring in the red and blue parts of the spectrum.[25] The spectral efficiency of photosynthesis is described by the plant action spectra, which quantifies the efficiency of conversion of incident photons of a given wavelength. A representative action spectrum is shown in figure 3a. Green light contributes less to photosynthesis due to the poor light absorption of chlorophyll in this region, however, it is required to some degree in order to allow for correct plant morphology.[26] Near infra red light contributes almost exclusively to the heating of the greenhouse environment and is not directly required for plant growth.[27] This region of the spectrum contains 52% of the energy within sunlight and therefore represents the most promising bandwidth to be harnessed by semi-transparent photovoltaic modules.[28] The relationship between the level of photosynthesis and crop growth is dependent on the specific crop as well as climatic conditions, however, a general rule often used is that a 1% drop in photosynthesis (such as by restriction of light reaching the plant) will result in a 1% fall in crop production for most greenhouse crops, such as tomatoes.[29]

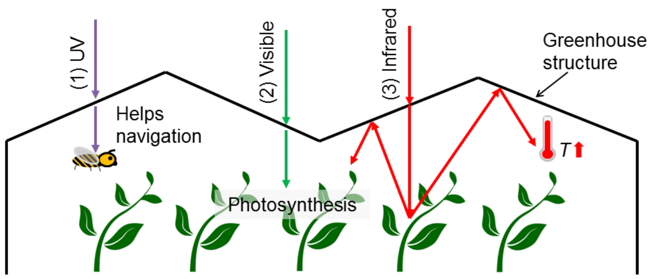

Fig. 2 Cartoon of the effect of light on greenhouse crop production: 1. UV light allows pollinating insects to navigate but also encourages certain fungi and diseases; 2. Visible light is used for photosynthesis and also heats the greenhouse; 3. Infrared light heats the greenhouse.

In order to assess the impact of transparent solar cells on plant growth, the averaged action spectrum of 27 herbaceous plants (including common greenhouse crops; tomatoes, lettuce and cucumbers) was used.[25] Figure 3a shows the photon flux density, $b_s(\lambda)$, and the photon flux density weighted by the plant action spectrum, $b_s(\lambda)a(\lambda)$. This modified spectrum can be understood as the photon flux spectrum which is required for optimal plant growth.

The impact of the absorption by the OPV device on crop growth, was determined by calculating a crop growth factor, $G(x)$ as a function of active layer thickness, x. We define this as,

$$G(x) = \frac{\int T(x,\lambda)b_s(\lambda)a(\lambda)d\lambda}{\int b_s(\lambda)a(\lambda)d\lambda}, \quad (1)$$

where $T(x,\lambda)$ is the total transmission of the complete simulated solar cell stack, which is governed by the thickness, x, of the active layer. The rate of photosynthesis in a crop is governed by the integral of the solar spectrum and action spectra, as seen in the denominator of equation 1. $G(x)$ therefore represents the ratio of the rate of photosynthesis under a clear sky and the rate under a greenhouse material (such as an OPV covering) with spectrally dependent transparency $T(x,\lambda)$. The growth of crops in the greenhouse is subsequently assumed to be reduced by 1% for every 1% reduction in the rate of photosynthesis.[29] This metric allows for the balance between crop growth and electricity production to be analysed but only applies for crops which benefit most from increased sunlight. For other crops, such as basil or poinsettia, lower light levels are desirable for the highest quality crops, and it has been shown that a 50% reduction in light has limited impact on some crop yields in certain climates.[30]

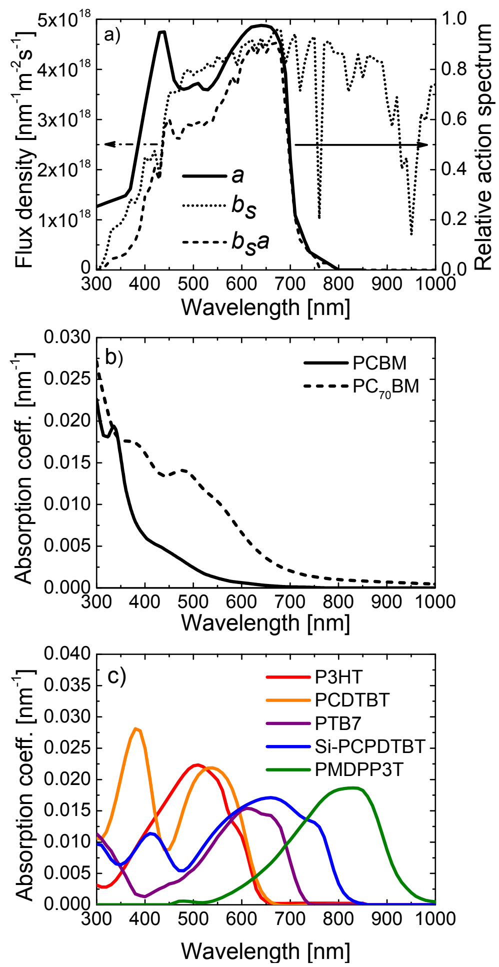

Fig. 3 a) relative action spectrum for plants (solid black line), AM1.5 photon flux density (dotted black line) and action spectrum modified photon flux density (dashed black line). b) Absorption coefficient for PCBM (solid black line) and $PC_{70}BM$ (dashed black line). c) Absorption coefficient for P3HT (solid red line), PCDTBT (solid orange line), PTB7 (solid purple line), Si-PCPDTBT (solid blue line) and PMDPP3T (solid green line). The absorption coefficients were calculated from the extinction coefficients for pristine polymer films given in the supplementary information.

2.2 Modelling electrical output

We use an optical model, together with empirical data and simple device physics to estimate the power conversion efficiency of a solar cell made from one of a number of polymer:fullerene blends as a function of transparency for optimal plant growth. The modelled device architecture is shown in figure 4.

We consider four commercially available polymer materials, namely poly (3-hexylthiophene) (P3HT), poly [N-

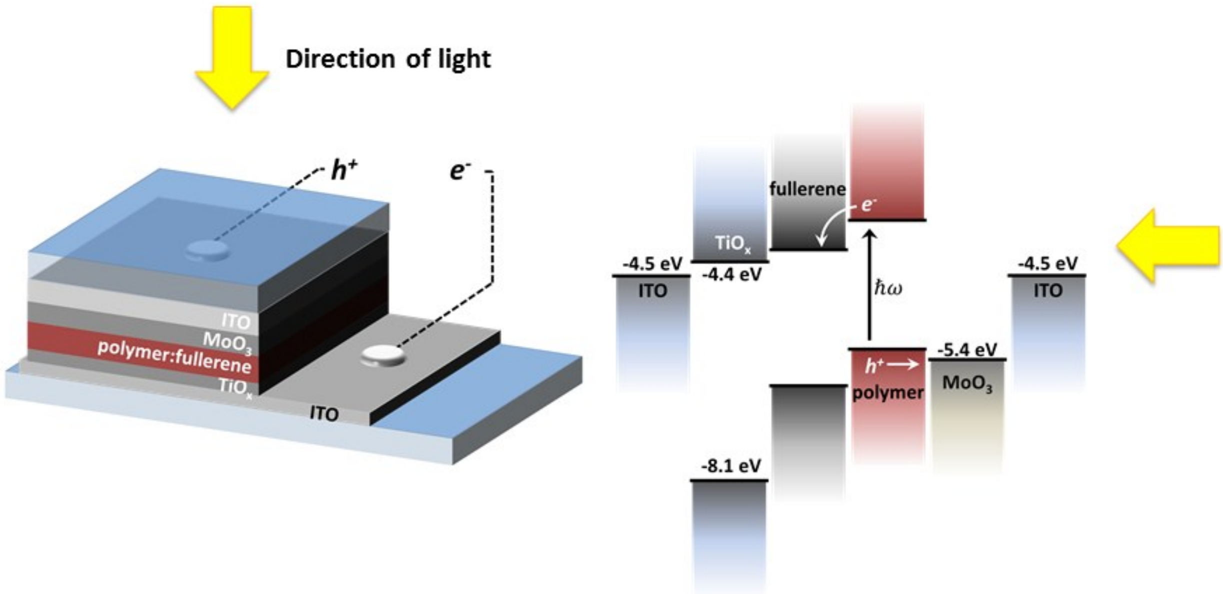

Fig. 4 Left: schematic of the solar cell device architecture used in this study: ITO/MoO_3/polymer:fullerene/TiO_2/ITO. For the optical modeling, a thick layer of glass (1.1 mm) was placed on either side of the solar cell in order to account for encapsulation. Right: energy level diagram for the modelled device. TiO_2 and MoO_3 are acting as hole- and electron blocking layers respectively.

900-hepta-decanyl-2,7-carbazole-alt-5,5-(40,70-di-2-thienyl-20,10,30-benzothiadiazole)] (PCDTBT), poly (4,8-bis[(2-ethylhexyl)oxy]-benzo[1,2-b:4,5-b]dithiophene-2,6-diyl3-fluoro-2-[(2-ethylhexyl)carbonyl]thieno[3,4-b]thiophenediyl) (PTB7) and poly [(4,40-bis(2-ethylhexyl)dithieno[3,2-b:20,30-d]silole)-2,6-diyl-alt-(2,1,3-benzothiadiazole)-4,7-diyl] (Si-PCPDTBT). Along with the commercially available materials, the low band gap polymer poly[[2,5-bis(2-hexyldecyl- 2,3,5,6-tetrahydro-3,6-dioxopyrrolo[3,4-c]pyrrole-1,4-diyl]-alt- [3,3-dimethyl-2,2:5,2- terthiophene]-5,5-diyl] (PMDPP3T) was also studied due to its high transparency at visible wavelengths and good device performance. These polymers are studied in blends with either 6,6-phenyl C61- butyric acid methyl ester (PCBM) or 6,6-phenyl C71-butyric acid methyl ester ($PC_{70}BM$). $PC_{70}BM$ is usually employed to enhance the absorption in the spectral region not covered by the polymer, resulting in higher efficiencies but reducing transparency in the visible region of the spectrum. Polymer:fullerene blend ratios were chosen from ratios shown in the literature to give high efficiencies for both regular and inverted device structures.[31–40]

In order to model the short circuit current density, J_{sc}, we employ a transfer matrix model according to Pettersson et al.[41] and implemented using genpro1 in ASA.[42] The model calculates the electric field propagating through a multilayer structure and hence the absorption in the following active layers and interlayers, along with the reflection from interfaces between each layer. The refractive index and complex refractive index data for the commonly studied blends (P3HT:PCBM (1:1), PCDTBT:$PC_{70}BM$ (1:4), PTB7:$PC_{70}BM$ (1:1.5), Si-PCPDTBT:$PC_{70}BM$ (1:1.5) and PMDPP3T:PCBM (1:3)) have previously been reported in the literature[40,43–48] and the indices for the lesser studied blends (P3HT:$PC_{70}BM$ (1:1), PCDTBT:PCBM (1:4), PTB7:PCBM (1:1.5), Si-PCPDTBT:PCBM (1:1.5) and PMDPP3T:$PC_{70}BM$ (1:3)) were calculated using Bruggemans model.[49,50] All complex refractive index data are presented in the supplementary information.

An internal quantum efficiency (IQE) of 100% has been shown to be possible in thin (active layer of 80 nm) devices made from PCDTBT:$PC_{70}BM$.[33] The model therefore assumes that all absorbed photons will contribute a single electron and a single hole for electrical conduction, i.e., the IQE is 100% across the spectrum. At zero bias, all absorbed photons will then contribute to the J_{sc}. It is further assumed that the fill factor, FF, for all the calculated solar cells is 70%. The open circuit voltage, V_{oc}, for each device architecture is obtained from *J*-*V* curves, measured under simulated solar irradiance, of the studied device blends from the literature (table 1).[31–33,35–40]

2.2.1 Efficiency limits for available materials

The open circuit voltage of any solar cell is determined by the energetic separation between the quasi Fermi levels for electrons and

Table 1 Polymer:fullerene blends and experimentally determined values for the V_{oc} of the respective blends, along with energy levels of materials presented in this study and band-gaps (determined from the absorption onset). Note that blends of a polymer with PCBM or PC70BM result in a similar V_{oc}, thus this same V_{oc} value was used for both fullerenes.

Material	Empirical V_{oc} [V]	Blend ratio	HOMO [eV]	LUMO [eV]	Bandgap [eV]
P3HT[51]			-5.1	-3.0	1.96
PCDTBT[33,35]			-5.5	-3.6	1.94
PTB7[36,39]			-5.2	-3.3	1.72
Si-PCPDTBT[37,38]			-5.3	-3.6	1.5
PMDPP3T[34,40]			-5.2	-3.9	1.3
PCBM[52]			-6.0	-3.7	2.3
$PC_{70}BM$[52]			-6.0	-3.7	2.3
P3HT:PCBM[31,32,53]	0.60	(1:1)			
PCDTBT:$PC_{70}BM$[33,35]	0.90	(1:4)			
PTB7:$PC_{70}BM$[36,39]	0.75	(1:1.5)			
Si-PCPDTBT:$PC_{70}BM$[37,38]	0.55	(1:1.5)			
PMDPP3T:PCBM[40]	0.60	(1:3)			

holes, and this separation is ultimately limited by the band gap in conventional solar cells or, in the case of organic heterojunction solar cells, by the energetic difference between the HOMO of the donor and the LUMO of the acceptor, sometimes called the electrical gap. For unconcentrated sunlight, the V_{oc} is always substantially lower than the electrical gap or band gap both in the case of organic and inorganic solar cells. The exact difference between band gap and V_{oc} varies between different materials and depends on the amount of non-radiative recombination and on the shape of the absorption edge.[54] For the case of organic solar cells, qV_{oc} typically lies some 300-400 meV below the electrical gap as probed by electroluminescence or photocurrent spectroscopy.[55–57] qV_{oc} has also been correlated to the value of HOMO(A)-LUMO(D) where the energy levels are probed by cyclic voltammetry and photoelectron spectroscopy,[51] but this method is subject to large uncertainties in the HOMO and LUMO energies.

The experimentally reported energy levels are shown in table 1 alongside empirical V_{oc} values. The data show the expected correlation between HOMO(A)-LUMO(D) and qV_{oc}. Table 1 also shows that as the donor materials increase their absorption in the infrared, the resulting raise of the LUMO level results in a lower V_{oc}. This supports the assumption that a certain threshold between the LUMO of the donor and the LUMO of the acceptor is needed for efficient charge separation. Therefore, only adjustment of the HOMO of the donor polymer is possible to lower the band gap and thus limiting the obtainable V_{oc} and hence efficiency of these low band-gap materials. However, the development of novel acceptor materials, with higher HOMO levels, could overcome this problem.

The correlation between HOMO(A)-LUMO(D) and qV_{oc} can also be used to estimate the V_{oc} that might be available from a new material, assuming that non-radiative losses remain similar to an existing benchmark. In the present context, this approach could be used to design OPV-greenhouse systems with the maximum net performance for any given spectrum required by the crop.

2.2.2 Choice of materials The transparency of a solar cell device is greatly impacted by the interlayer and electrode materials used. In our simulations, the device architecture and contact materials were chosen for their high transparencies and potential for large scale production. In this study, a front contact of molybdenum trioxide (MoO_3) coated onto tin-doped indium oxide (ITO) of 30 nm and 70 nm respectively was chosen. MoO_3 is a commonly used material for inverted solar cells and has been shown to offer good hole collection and electron blocking properties. Even though ITO is a very expensive material (which requires vacuum deposition, greatly increasing costs[58]) and much effort is being put into removing the need for ITO as a transparent material in organic photovoltaics and organic light emitting devices,[59] alternative materials which offer similar transparency and conductivity have not been demonstrated on large area substrates. Ag-NWs has been proposed as a potential candidate to replace ITO, as this material has shown high transparencies along with low sheet resistances and costs.[58,60,61] However, relevant optical data for sufficiently transparent electrode materials could not be found for use in this study.

For the back contact we use a hole blocking interlayer of 30 nm TiO_2 with a 70 nm electrode layer based on the optical and electrical properties of ITO. This results in a device using ITO for both electrodes which does not correspond to any real cell architecture. However, since only the optical absorption and transmission, as well as electrical conductivity of these layers are relevant for our modelling, ITO provides appropriate proxy for a generalised assumption of electrode characteristics. The thickness of the active layer of polymer and fullerene blends, x, is allowed to vary in order to achieve optimal absorption as a function of the transparency. The device is illuminated from the ITO/MoO_3 contact.

The largest contribution from the non-active layers to the device absorption spectrum is the MoO_3 (see supplementary information). The MoO_3 absorbs primarily in the violet region (300 400 nm), and since plants utilise little of the light in this region (see section 2.1), the primary implication with the MoO_3 absorption will be the decrease in the J_{sc} due to less absorption in the active layer in that spectral region, rather than any major impact on crop growth. TiO_2 is however the contact material with the highest absorption in the spectrum, but since TiO_2 is used as the back contact interlayer and most light between 300 - 400 nm is already being absorbed by the front contact and the fullerenes, the primary decrease in performance due to TiO_2 will be due to a minor reduction in device transparency, although this has little impact on crop growth due to the low wavelength of TiO_2 absorption. Commonly used alternative interlayer materials, such as PEDOT:PSS would result in greater impacts on both the device transparency and efficiency due to less light reaching the active layer.

From figure 3b it is seen that the choice of fullerene greatly impacts the transparency of the device. The larger $PC_{70}BM$ fullerene absorbs much more within the PAR region than PCBM. However, the larger absorption in the higher energy region of the spectrum observed for $PC_{70}BM$ could mean that a thinner active layer is needed in order to obtain sufficient efficiency. The choice of fullerene expected to play a key role particularly in the case of PCDTBT: fullerene (1:4) and PMDPP3T:fullerene (1:3) blend since the fullerenes acts as major absorbers. For this reason, the fullerene acceptor molecules, in conjunction with carefully selected polymer donors (figure 3c), can be combined to provide an optimal absorption profile for device efficiency along with levels of transparency required for plant growth.

The absorption spectra of the five polymers shown in figure 3c show that P3HT absorbs primarily within the PAR region, suggesting devices using this material will likely greatly impact crop growth, despite the peak in P3HT absorption coinciding with a slight dip in the action spectra (in the green, where plants absorb less). Contrary to P3HT, PCDTBT shows two profound absorption peaks namely around 400 nm and 580 nm, with a reasonable absorption between the two characteristic absorption peaks of plants. PTB7 shows absorption peaks around the largest peak in the action spectrum and in the UV, but allows for transparency in the rest of the spectrum (350 nm - 500 nm). Si-PCPDTBT shows three profound absorption peaks, namely below 300 nm, at 400 nm and at 650 nm. It shows a large absorption in the infra-red, allowing for high absorption without affecting the plant growth. The two primary absorption peaks at 400 nm and 650 nm do, however, coincide with the characteristic peaks for plant growth. The low band gap polymer, PMDPP3T shows a large peak around 800 nm which tails off in the PAR, allowing for good transparency for plants. A very small peak around 500 nm is also seen, which is expected to slightly increase the total device efficiency whilst having minimal impact on transparency in the PAR.

3 Results

Figure 5a shows the crop growth factor (equation 1) as a function of the active layer thickness. The maximum achievable crop growth factor was found to be around 88% for an extremely thin active layer ($\sim$ 5 nm), given the choice of contact materials (ITO/MoO_3 front contact and TiO_2/ITO back contact). It is seen that films made with PCBM fullerene acceptors will in all cases be more transparent than those made with the same weight ratio of $PC_{70}BM$ (at a specific thickness) due to the greater absorption of the $PC_{70}BM$ in the 400 nm to 700 nm region.

Figure 5 shows the greatest transparency is obtained using the low band gap PMDPP3T polymer due to the window of transparency between 300 nm to 600 nm. Figure 5b shows the short circuit current density, J_{sc}, as a function of the active layer thickness. P3HT and PCDTBT blends are seen to absorb the least photons owing to their relatively high band gap, allowing only for absorption below around 650 nm, and correspondingly yield low J_{sc}'s. PTB7 is seen to generate an intermediate magnitude of current, and Si-PCPDTBT and PMDPP3T are seen to generate the most current due to their low band gaps. Furthermore, it is observed that blends with the larger $PC_{70}BM$ fullerenes (dashed lines) will in all cases generate more current for a given device thickness, due to the increased absorption of the fullerene in the visible region.

Figure 6 shows the growth factor, G, as a function of the estimated power conversion efficiency (PCE). Despite PTB7 and Si-PCPDTBT devices showing a higher J_{sc} due to higher absorption than the PCDTBT devices, the smaller V_{oc} of PTB7 (0.75 V) and the very small V_{oc} of Si-PCPDTBT (0.55 V) means that the overall G as a function of PCE is quite low. In the case of P3HT, a low current and a low V_{oc} results in low performance. The large V_{oc} of PCDTBT:fullerene devices (0.9 V) resulted in a very large G as a function of PCE even though the absorption of these blends is inferior than all other blends. The largest overall G as a function of PCE is however observed for PMDPP3T (except within a small region where PCDTBT performs similarly). For all blends studied it is observed that the improved absorption gained when using the more expensive $PC_{70}BM$ compared to PCBM is not beneficial due to the reduction in transparency of the device. The opportunity to utilize PCBM in the most optimum devices, instead

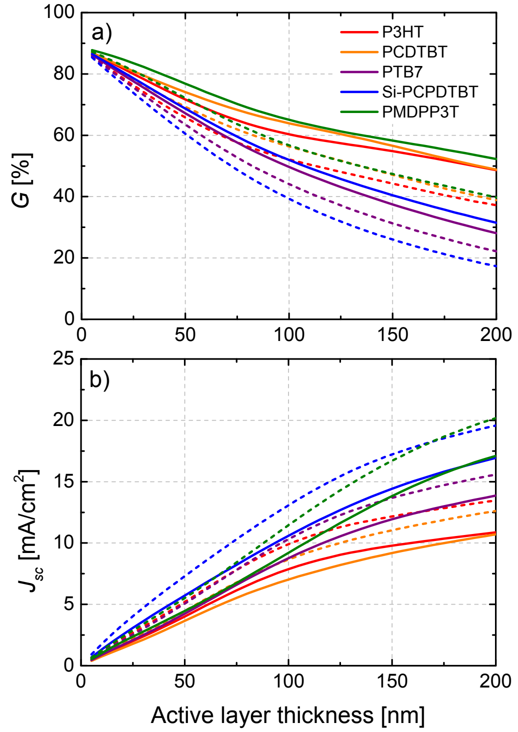

Fig. 5 a) crop growth factor, G, and b) short circuit current density, J_{sc}, as a function of active layer thickness calculated from the optical modelling. The solid lines represents the polymer:PCBM blends and the dashed lines the polymer:$PC_{70}BM$ blends. Blend ratios of P3HT:fullerene (1:1), PCDTBT:fullerene (1:4), PTB7:fullerene (1:1.5), Si-PCPDTBT:fullerene (1:1.5) and PMDPP3T (1:3) were studied. The modelled devices were illuminated from the MoO_3 contact.

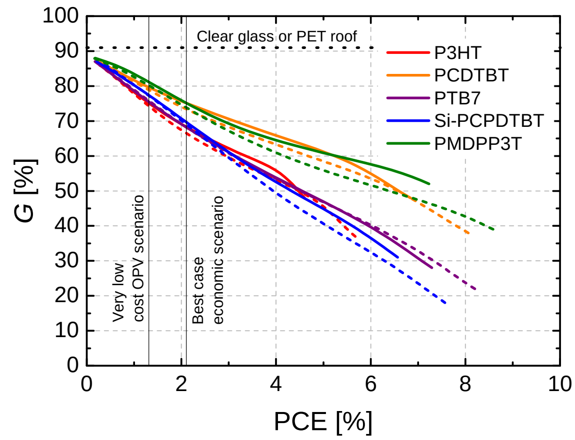

Fig. 6 Crop growth factor, G, as a function of the power conversion efficiency, PCE, for active layers ranging between 5 nm and 200 nm. Solid lines are blends with PCBM and dashed lines are blends with $PC_{70}BM$ in the ratios of P3HT:fullerene (1:1), PCDTBT:fullerene (1:4), PTB7:fullerene (1:1.5), Si-PCPDTBT:fullerene (1:1.5) and PMDPP3T:fullerene (1:3). The fill factor was set to 70% in all cases, and the V_{oc} was set according to empirical values found in the literature, see table 1. The modelled devices were illuminated from the MoO_3 contact. Straight vertical lines indicate the efficiencies required for an OPV greenhouse to be economically justified, as discussed in the following section.

of $PC_{70}BM$, could greatly reduce the cost of modules.

Counter-intuitively, figure 6 shows that low band-gap polymers do not always outperform polymers which absorb strongly in the PAR. PCDTBT:fullerene blends can demonstrate similar performance in a greenhouse application compared with lower band-gap polymers, due to the high efficiency (largely resulting from the high V_{oc}) of PCDTBT based blends being able to compensate for low PAR transparency. In the case of the comparison between PCDTBT and PMDPP3T shown here, this is principally due to the reduced V_{oc} which low-band-gap materials necessitate when used in blends with PCBM or PC70BM.

4 Economic Analysis

In order to assess the potential of an OPV greenhouse, an economic analysis of such a system was conducted. The economic analysis of the photovoltaic greenhouse is based on a multi-span structure with a planar roof angled at 23° (as shown in figure 2), located in southern Spain. The south facing roof is covered in photovoltaic modules, with the remainder of the structure consisting of plastic sheeting over a steel frame. Costs for the installation include all balance of system (inverter, labour etc. See supplementary information for details) and replacement costs over a 10 year time-frame.[62] A 10 year time-frame is chosen, since OPV has a relatively short lifetime, and thus the system time-frame is set at the expected lifetime of major electrical components such as the inverter. This analysis is based on the added costs of including PV in a greenhouse and thus does not include the greenhouse structure itself or the plastic sheeting which would be required regardless of whether PV was present on the greenhouse.

Such analysis has a strong dependency on the cost of the OPV module. The cost of modules is heavily dependent on the cost per square metre rather than the level of efficiency, due to costs being dominated by non-active layers.[63] This analysis used baseline and optimistic scenarios for the cost per square metre of photovoltaic module, and assumed an equal cost applied regardless of the efficiency of the module. These values were based on the most promising materials shown in reference 58, assuming a degree of cost reduction due to scale-up in the manufacture of the technology. A final scenario was considered to account for the possibility of OPV achieving extremely low costs, as projected by reference 18 (which is in close agreement with reference 63).

A model was developed to compute a Net Present Value (see SI[64]) for the photovoltaic greenhouse, based on the assumptions described above combined with an assumed economic environment. The results of this analysis are shown in table 2. For each scenario, the model calculated the minimum efficiency of the photovoltaic module which gave a Net Present Value, over a ten year time-frame, of zero. This was then translated to a cell efficiency by considering that 85% of the module constitutes functioning cells, as has been seen in large scale OPV modules using laser patterning techniques.[65]

The results of the economic analysis (table 2) show that in the baseline scenario, where OPV modules remain reasonably expensive, a cell efficiency of 10.2% (equating to a module cost of 0.46 $€/W_p$) would be required for a PV greenhouse to be economically justified. This is far in excess of the efficiencies achievable with the materials studied in this work, whilst insuring limited impact to crop growth, as seen in figure 6. The Best Case and Very Low Cost OPV scenarios both result in greatly reduced device efficiencies, of 2.1% and 1.31%, for an OPV greenhouse to make financial sense. Reference to figure 6 shows that such efficiencies could be achieved with all the polymers studied, including the comparatively poorly performing P3HT, whilst ensuring crop production is not reduced by more than 30%. This also suggests that the active layer thickness of such devices would be less than 40 nm, in order to reach the levels of transparency and efficiency required. The results of the Best Case and Very Low Cost OPV scenarios also show that OPV cost targets of 1.71 $€/W_p$ and 0.53 $€/W_p$ respectively would be required, values which are both either already achievable or projected, at least for P3HT based modules.[18,62,63]

4.1 Global Scalability of PV Greenhouses

Plastic and glass represent the principle materials for greenhouse structures worldwide. Both of these materials can be used as a substrate for OPV technology, making it a potentially simple matter to replace such materials with photovoltaic surfaces. In order for PV greenhouses to make economic sense, the greenhouse structure should outlast the module, i.e. more than 5 years for the case of OPV, or longer for inorganic technologies. Currently, much of the global greenhouse capacity is based on reasonably primitive structures such as low quality plastic sheeting covering a steel frame. Such structures require the sheeting to be changed regularly and are subject to heavy degradation each growing season. However, as agricultural industries develop and become more sophisticated worldwide, greenhouse structures are likely to also become more robust and thus represent more suitable constructions on which to mount PV modules.

Figure 7 shows the potential solar electricity generating capacity of the worldwide greenhouse area. This assumes durable greenhouses become the norm worldwide and is based on assumptions of typical insolation and greenhouse design (i.e. roof inclination) for each region. This shows that if all polytunnels in China could be transformed into PV greenhouses, the 415 GW_p of PV capacity this could provide, would supply almost 15% of the national electricity demand. In Spain and Turkey, this figure would be around 6% of the national electricity demand, contributing significantly to greenhouse gas emission reductions.

5 Discussion

5.1 Materials for OPV Greenhouses

OPV technology may represent a unique solution for PV greenhouses by providing easily installable PV systems whilst maintaining the productivity of agricultural land. OPV materials show the potential for limited impact on crop growth, particularly in the case of polymers which show minimal absorption in the PAR, such as PMDPP3T. However, we have also shown that optical absorption within the PAR region by organic semi-conducting polymers is not a barrier to their application in a PV greenhouse, as very thin devices can allow sufficient transparency, provided such materials yield high efficiency devices (as in the case of PCDTBT). However, significant absorption of PAR in ancillary materials means that all device structures will have some impact on crop growth, irrespective of the active layer absorption. The situation could be significantly improved with the development of contacts with increased transparency, both to increase efficiency and reduce the impact on crops.

Polymers with low extinction coefficients often result in poor OPV devices due to the need for very thick devices which subsequently suffer high recombination losses due to poor charge transport. In contrast, the requirements of an OPV greenhouse mean that such materials could be well suited to this application. Many materials studied in this work would require extremely low thicknesses in order to maintain the required level of transparency, and this may lead to difficulties in manufacture. However, thicker devices which could be more easily manufactured (i.e. with an active layer of more than 50 nm) could be made using material combinations with broad absorption spectra but low extinction coefficients,

Table 2 Inputs and results of an economic analysis of an OPV greenhouse showing cell efficiencies required to achieve a Net Present Value of zero over a ten year period

Variable	Best Case	Baseline	Very Low Cost OPV
Discount Rate	2%	6%	6%
Lifetime	10 years	5 years	5 years
Module Cost	30 €/m^2	40 €/m^2	5.87 €/m^{2*}
Performance Ratio	85%	80%	80%
Insolation	2200 W/m^2	2200 W/m^2	2200 W/m^2
Value of Electricity	0.159 €/kWh [1]	0.095 €/kWh [2]	0.095 €/kWh
Annual Increase in Electricity Value (above inflation)	0%	3%	3%
Minimum Cell (Module) Efficiency	2.1% (1.75%)	10.2% (8.63%)	1.31% (1.11%)

[1] Spanish feed-in-tariff for building integrated projects; [2] Price of electricity for a commercial consumer in Spain

such as PCDTBT:PCBM, whilst maintaining the high levels of transparency required.

The more expensive $PC_{70}BM$ is often used in OPV blends to give higher efficiencies, due to the higher absorption of this larger fullerene, compared with the lower cost PCBM. This work demonstrates that the use of $PC_{70}BM$ provides no advantage in a PV greenhouse application as the increased efficiency is outweighed by the lower transparency in the PAR.

In order to justify higher costs per square metre for OPV modules, higher efficiencies are required. Using lower transparency but higher efficiency devices could be well suited to use on greenhouses growing speciality crops which require lower light levels, such a tropical flowers, which can withstand around a 50% reduction in light in certain climates.[30] Alternatively, lower band-gap materials or tandem cells with polymer materials absorbing either side of the PAR could increase efficiencies without impacting crop growth. However, low band-gap materials are limited by the increasingly poor V_{oc} which results from the LUMO level of the fullerene acceptor, unless alternative acceptor materials with lower LUMO levels can be found.

5.2 OPV vs. Mature PV Greenhouses

As discussed in section 1, mature PV technologies have been used with some success within PV greenhouses. Through the use of large gaps between cells, opaque crystalline or thin-film cells can create a see-through module, with the degree of transparency being determined by the level of coverage of the cells. Figure 8 shows a comparison of such an approach with semi-transparent OPV technology, as modelled in this work, as well as semi-transparent amorphous silicon technology. This assumes opaque crystalline silicon cells with a cell efficiency of 20% and opaque CIGS modules of 12% efficiency, under an insolation of 2200 kWh/m^2 and a performance ratio of 80%. The green shaded area shows a semi-transparent $PMDPP3T : PC_{60}BM$ based device ranging in thickness from 1-200 nm, and covering from 0-100% of the greenhouse roof.

A typical greenhouse in Northern Europe consumes between 20 MWh/ha/year and 70 MWh/ha/year of electricity.[69] Figure 8 shows that all PV technologies can provide sufficient electricity, on an annual average basis, to meet all the requirements of greenhouse agriculture with minimal impact to crop growth. Although electricity is only 10-30% of the energy requirement of a greenhouse,[69] electricity generated on a greenhouse structure also holds substantial value through exporting clean energy to the grid.

Due to the low efficiencies seen for semi-transparent modules, figure 8 shows that in terms of energy density, OPV provides no advantage over mature, opaque crystalline silicon PV technology with partial roof coverage. This demonstrates the need for high efficiency polymers and ultra-transparent ancillary OPV materials which can provide increased efficiencies without impacting crop growth. Such high transparency OPV contact materials would result in the shaded green area in figure 8 moving further up the y-axis. If contact materials with 100% transparency in the PAR region could be developed, the left most point of solid green line at the bottom of the shaded area of figure 8 would reach close to the top of the y-axis, placing the shaded area largely above the crystalline silicon line, and showing the advantage of OPV of all opaque technologies. These results shows that some already available semiconducting polymers used in OPV, such as PMPDPP3T and PCDTBT, have the potential to perform better than some thin-film technologies, such as flexible CIGS, in this application.

Other properties of OPV, such as low weight and flexibility could, however, give the technology an advantage over rigid crystalline silicon modules in the ease of which it could be implemented within a plastic (rather than glass) greenhouse, which comprise the vast majority of greenhouses worldwide. OPV technology could make retro-fitting of existing greenhouses (which may not be capable of supporting the weight

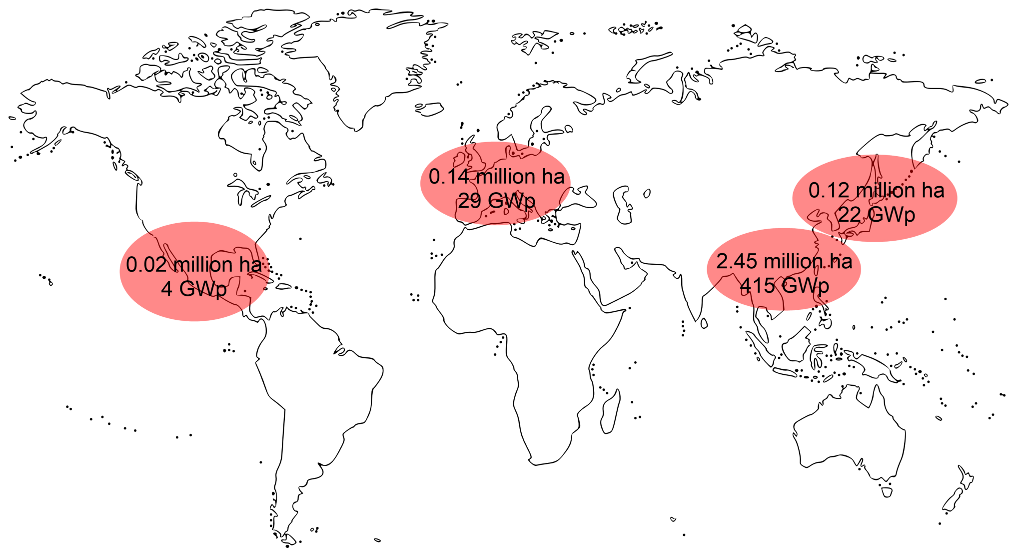

Fig. 7 The global potential OPV greenhouses assuming 5% efficient OPV modules. Figures represent the countries with the highest reported levels of greenhouse area in the region, namely: Mexico and the US in America[66]; Spain, Turkey, Italy, Netherlands and France in Europe[66,67]; Japan and North Korea in Northern Asia[66]; and China.[68]

of crystalline silicon modules) possible, potentially using fast deployment techniques as demonstrated in reference 17. Additionally OPV could be implemented through a roll-able screen, which would allow for OPV modules to be removed when light levels are lower, such as in the winter, thus reducing impacts on crop growth. This could allow the OPV modules to act as a NIR screen, which have been shown to reduce energy demands of greenhouses without reducing yields, if used for certain periods of the year[27]. If the modules were removed for 5 months over the winter months, the electricity yield would be reduced by around 35% (for a system located in Southern Spain) as well as potentially accelerating degradation due to mechanical stress from moving the module. Thus such a situation would significantly impact the economics of the installation. However, thin-film technologies, such a CIGS also have similar flexible properties and perform almost as well as the best OPV device in a greenhouse application, as seen in figure 8.

5.3 OPV Greenhouse Economics

Table 2 shows that when considering the most optimistic assumptions, module efficiencies would need to be in the region of 2%, a value already achievable in large area modules.[70] However, considering a more pessimistic economic and technological environment, efficiencies close to the hero cells currently seen in the lab would be required, a challenging prospect for the technology, particularly if there is a need to maintain transparency of the module. However, if the huge cost reductions which are hoped for OPV are realised, very low efficiencies could still prove to be economically attractive, as seen in the *Very Low Cost OPV* scenario in table 2. A comparison of figure 6 with table 2 shows that achieving the required efficiencies to make this application economically viable could already be achievable even with the worst performing material modelled in this work, P3HT, whilst incurring less than a 30% reduction in crop growth .

By placing an economic value on the crops grown in an OPV greenhouse, the optimum level of OPV transparency could be determined. However, since most crops grown in polytunnels are fruit or vegetable crops, the nature of the produce, such as the size or shape, greatly impacts its value. The formation of fruits within a crop depends on the nature of the light within the greenhouse, and the effect differs between different crops and between seasons and climates. Therefore, any such trade-off would need to take such factors into account, which is beyond the scope of this work.

In addition, electricity provided by an OPV greenhouse may have an increased value if it enabled climate controlled agriculture, such as providing water pumping (or even desalination) and other automated processes in a location far from grid lines. Table 2 assumes grid connected installations, however, off-grid electricity is often far more expensive as alternatives are limited to renewable power such as wind or solar, or diesel generators. In such a case, the economics of a PV greenhouse would be likely to be greatly improved despite added requirements for battery storage systems, resulting in even lower OPV efficiencies being required for the application to be economically justified.

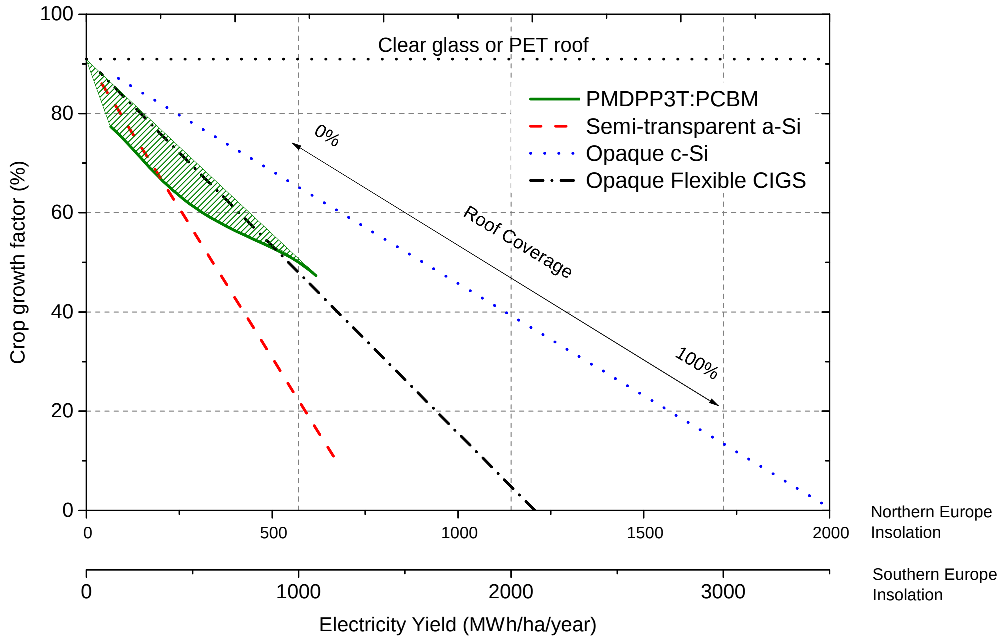

Fig. 8 PV electricity generation against impact on crop growth for differing levels of roof coverage and for both OPV and mature PV technologies. X-axes show electricity output assuming insolation of 2200 kWh/m^2 (representative of Southern Europe) and 1300 kWh/m^2 (Northern Europe), including a performance ratio of 80% for all cases and a module active area of 85% for OPV technologies. Data on transparency and PV efficiency for OPV was based on the model described in this work and from amorphous silicon from [13]. Opaque crystalline silicon cells are assumed to be 20% efficient and flexible CIGS modules 12% efficient. The green shaded area shows modules using a blend of PMDPP3T:PCBM with a range of device thicknesses

6 Conclusions

Photovoltaic greenhouses are a niche application which could allow vast areas of the world to produce both food and sustainable energy. The availability of a wide array of semiconducting polymer materials provides OPV with the potential to harness light not required for plant growth. Organic semiconductor materials are unique in this respect due to their tunable finite bandwidth absorption, and tandem devices could allow a number of different regions of the spectrum to be absorbed.

Through modelling the impact of semi-transparent OPV modules on crop growth for a variety of commercially available organic semi-conductor materials, we have shown that OPV materials are currently not unique in being able to generate substantial electricity with limited impact to crops in a PV greenhouse. We show that currently available materials absorb too much light within the photosynthetically active spectrum to prove to be an improvement over spaced out opaque modules based on more efficient, inorganic materials such as crystalline silicon. However, a low-band gap polymer, PMDPP3T, as well as a high efficiency mid-band-gap polymer, PCDTBT, both show improved performance in a greenhouse application in comparison to opaque CIGS modules. Additionally, the light-weight, flexible nature of OPV technology may prove to be an advantage for the technology in this application, thus providing a potentially unique solution for rapidly retro-fitting existing greenhouse strucutures, if these high performing materials can be produced at a low enough cost.

This analysis demonstrates that avoiding absorption within the region of the spectrum required for crop growth is not the most important factor for an OPV material to be suitable for a greenhouse application. Instead higher efficiency semiconductor materials and very high transparency contact materials are a more important requirement. It is also shown that the use of larger fullerenes which typically yield higher efficiency devices, provide no benefit in a greenhouse application due to the higher absorption in the region of the spectrum required for crop growth.

Economic modelling of an organic photovoltaic greenhouse shows that the efficiencies required for OPV to be economically viable in this application can already be achieved, even with the very common OPV material, P3HT, whilst impacting crop growth by less than 30%, based on optimistic assumptions for technology development and/or economic environment. On the other hand, taking pessimistic assumptions for OPV costs and the economic environment for PV, efficiencies close to those of hero cells seen in the lab would be required (whilst also maintaining high transparency), for an OPV greenhouse to be economically justified. However, the economics of a PV greenhouse could be greatly improved in off-grid scenarios where electricity is far more valuable. In addition, lower levels of transparency (which could allow thicker and hence more efficient modules) could be tolerated if speciality crops such as basil or tropical flowers are being grown.

7 Acknowledgements

The authors would like to thank Dr. Lee Richter (NIST) for providing the refractive index data for PTB7 used in this manuscript. CJME would like to acknowledge support from the Grantham Institute - Climate Change and the Environment and Climate-KIC through a PhD studentship. JN would like to acknowledge support from the Royal Society through an Industrial Fellowship. MCQ acknowledges financial support from the Ministerio de Economia y Competitividad through project MAT2012-37776. AU acknowledges financial support from MINECO-Spain, Grant ENE2013- 48816-C5-3-R, including Feder Funding.

References

1 C. Dupraz, H. Marrou, G. Talbot, L. Dufour, A. Nogier and Y. Ferard, *Renewable Energy*, 2011, **36**, 2725–2732.
2 Headway Solar, *Harvesting Crops Along with Sunshine: Utilization of solar power plant land for crop cultivation*, 2014.
3 Belectric, *BELECTRIC PV-Greenhouses: All-in-One greenhouse solutions*, Belectric technical report, 2011.
4 C. Campiotti, C. Bibbiani, F. Dondi, M. Scoccianti and C. Viola, *Journal of Sustainable Energy*, 2011, **II**, 51–56.
5 M. Kadowaki, A. Yano, F. Ishizu, T. Tanaka and S. Noda, *Biosystems Engineering*, 2012, **111**, 290–297.
6 G. Minuto, F. Tinivella, C. Bruzzone and A. Minuto, *Informatore Agrario Supplemento*, 2011, **50**, 1–5.
7 S. Eleuteri, *Photon International*, 2009, 56–60.
8 J. Pérez-Alonso, M. Pérez-García, M. Pasamontes-Romera and A. Callejón-Ferre, *Renewable and Sustainable Energy Reviews*, 2012, **16**, 4675–4685.
9 G. Minuto, Energy Day - SERRE APERTE ALLENERGIA: dal vetro fotovoltaico alla serra energeticamente indipendente.
10 P. J. Sonneveld, G. L. A. M. Swinkels, B. A. J. V. Tuijl, H. J. J. Janssen, J. Campen and G. P. A. Bot, *Solar Energy*, 2011, **85**, 432–442.
11 Basque Research, *ULMA and Tecnalia conduct crop testing with a special photovoltaic panel for greenhouses*, 2012, `http://www.basqueresearch.com/berria\_irakurri.asp?Berri\_Kod=3697\&hizk=I\#.UIFOmMXA\_Sh`.
12 Konarka, *Case Study Brookdale Fruit Farm Greenhouse Project*, 2012.
13 Sun Well Solar, PV EXPO 2011, Taiwan Forum, 2012.
14 S. Gavrila and A. Gonteau, *Programmable Devices and Embedded Systems*, 2010, **10**, 162–166.
15 P. J. Sonneveld, G. L. A. M. Swinkels, J. Campen, B. A. J. V. Tuijl, H. J. J. Janssen and G. P. A. Bot, *Biosystems Engineering*, 2010, **106**, 48–57.
16 C. J. M. Emmott, N. J. Ekins-Daukes and J. Nelson, *Energy & Environmental Science*, 2014, **7**, 1810–1818.
17 F. C. Krebs, N. Espinosa, M. Hösel, R. R. Søndergaard and M. Jørgensen, *Advanced Materials*, 2014, **26**, 29–39.
18 C. J. Mulligan, M. Wilson, G. Bryant, B. Vaughan, X. Zhou, W. J. Belcher and P. C. Dastoor, *Solar Energy Materials and Solar Cells*, 2014, **120**, 9–17.
19 *Heliatek GmbH*, `http://www.heliatek.com/`.
20 R. R. Lunt and V. Bulovic, *Applied Physics Letters*, 2011, **98**, 113305(3).
21 C.-C. Chen, L. Dou, R. Zhu, C.-h. Chung, T.-b. Song, Y. B. Zheng, C. E. T. Al and Y. Yang, *ACS Nano*, 2012, **6**, 7185–7190.
22 G. L. Yang Yang, *Transparent organic solar cells for agronomic applications*, 2014, `http://www.google.com/patents/WO2014131027A1?cl=en`.
23 R. R. Lunt, *Applied Physics Letters*, 2012, **101**, 043902.
24 N. Li, D. Baran, K. Forberich, F. Machui, T. Ameri, M. Turbiez, M. Carrasco-Orozco, M. Drees, A. Facchetti, F. C. Krebs and C. J. Brabec, *Energy & Environmental Science*, 2013.
25 K. Inada, *Plant & Cell Physiology*, 1976, **17**, 355–365.
26 M. Johkan, K. Shoji, F. Goto, S. Hahida and T. Yoshihara, *Environmental and Experimental Botany*, 2012, **75**, 128–133.
27 C. Stanghellini, J. Dai and F. Kempkes, *Biosystems Engineering*, 2011, **110**, 261–271.
28 P. J. Sonneveld, G. L. A. M. Swinkels, G. P. A. Bot and G. Flamand, *Biosystems Engineering*, 2010, **105**, 51–58.
29 L. F. M. Marcelis and A. G. M. Broekhuijsen, *Acta Horticulturae*, 2006, **711**, 97–104.
30 G. Minuto, *Risultati della sperimentazione nuove tecnologie di serre fotovoltaiche*, 2010.
31 G. Li, V. Shrotriya, J. Huang, Y. Yao, T. Moriarty, K. Emery and Y. Yang, *Nature Materials*, 2005, **4**, 864–868.
32 C. Waldauf, M. Morana, P. Denk, P. Schilinsky, K. Coakley, S. a. Choulis and C. J. Brabec, *Applied Physics Letters*, 2006, **89**, 233517(3).
33 S. H. Park, A. Roy, S. Beaupre, S. Cho, N. Coates, J. S. Moon, D. Moses, M. Leclerc, K. Lee and A. J. Heeger, *Nature Photonics*, 2009, **3**, 297–303.
34 J. C. Bijleveld, A. P. Zoombelt, S. G. J. Mathijssen, M. M. Wienk, M. Turbiez, D. M. de Leeuw and R. A. J. Janssen, *Journal of the American Chemical Society*, 2009, **131**, 16616–16617.
35 Y. Sun, J. H. Seo, C. J. Takacs, J. Seifter and A. J. Heeger, *Advanced materials*, 2011, **23**, 1679–1683.
36 Y. Liang, Z. Xu, J. Xia, S.-T. Tsai, Y. Wu, G. Li, C. Ray and Y. Luping, *Advanced Materials*, 2010, **22**, E135–E138.
37 M. Morana, H. Azimi, G. Dennler, H.-J. Egelhaaf, M. Scharber, K. Forberich, J. Hauch, R. Gaudiana, D. Waller, Z. Zhu, K. Hingerl, S. S. van Bavel, J. Loos and C. J. Brabec, *Advanced Functional Materials*, 2010, **20**, 1180–1188.
38 S. Albrecht, S. Schäfer, I. Lange, S. Yilmaz, I. Dumsch, S. Allard, U. Scherf, A. Hertwig and D. Neher, *Organic Electronics*, 2012, **13**, 615–622.
39 Z. He, C. Zhong, S. Su, M. Xu, H. Wu and Y. Cao, *Nature Photonics*, 2012, **6**, 591–595.
40 W. Li, A. Furlan, K. H. Hendriks, M. M. Wienk and R. A. J. Janssen, *Journal of the American Chemical Society*, 2013, **135**, 55295532.
41 L. A. A. Pettersson, L. S. Roman and O. Inganas, *Journal of Applied*

Physics, 1999, **86**, 487–496.
42 B. Pieters, J. Krc and M. Zeman, Photovoltaic Energy Conversion, Conference Record of the 2006 IEEE 4th World Conference on, 2006, pp. 1513–1516.
43 F. Monestier, J.-J. Simon, P. Torchio, L. Escoubas, F. Flory, S. Bailly, R. de Bettignies, S. Guillerez and C. Defranoux, *Solar Energy Materials and Solar Cells*, 2007, **91**, 405–410.
44 N. P. Sergeant, A. Hadipour, B. Niesen, D. Cheyns, P. Heremans, P. Peumans and B. P. Rand, *Advanced materials*, 2012, **24**, 728–32.
45 H. Azimi, M. Morana, T. Ameri, B. Dastmalchi, M. Scharber, K. Hingerl and C. J. Brabec, *Solar Energy Materials and Solar Cells*, 2011, **95**, 3093–3098.
46 M. Campoy-Quiles, J. Nelson, D. D. C. Bradley and P. G. Etchegoin, *Physical Review B*, 2007, **76**, 235206.
47 A. Guerrero, B. Drling, T. Ripolles-Sanchis, M. Aghamohammadi, E. Barrena, M. Campoy-Quiles and G. Garcia-Belmonte, *ACS Nano*, 2013, **7**, 4637–4646.
48 M. R. Hammond, R. J. Kline, A. A. Herzing, L. J. Richter, D. S. Germack, H.-W. Ro, C. L. Soles, D. A. Fischer, T. Xu, L. Yu, M. F. Toney and D. M. DeLongchamp, *ACS Nano*, 2011, **5**, 8248–8257.
49 T. Choy, *Effective Medium Theory: Principles and Applications*, Clarendon Press, 1999.
50 D. A. G. Bruggeman, *Annalen der Physik*, 1935, **416**, 636–664.
51 M. C. Scharber, D. Mühlbacher, M. Koppe, P. Denk, C. Waldauf, a. J. Heeger and C. J. Brabec, *Advanced Materials*, 2006, **18**, 789–794.
52 J. M. Frost, M. A. Faist and J. Nelson, *Advanced Materials*, 2010, **22**, 4881–4884.
53 W. Ma, C. Yang, X. Gong, K. Lee and A. J. Heeger, *Advanced Functional Materials*, 2005, **15**, 1617–1622.
54 T. Kirchartz, K. Taretto and U. Rau, *The Journal of Physical Chemistry C*, 2009, **113**, 17958–17966.
55 K. Vandewal, A. Gadisa, W. D. Oosterbaan, S. Bertho, F. Banishoeib, I. Van Severen, L. Lutsen, T. J. Cleij, D. Vanderzande and J. V. Manca, *Advanced Functional Materials*, 2008, **18**, 2064–2070.
56 M. A. Faist, T. Kirchartz, W. Gong, R. S. Ashraf, I. McCulloch, J. C. de Mello, N. J. Ekins-Daukes, D. D. C. Bradley and J. Nelson, *Journal of the American Chemical Society*, 2012, **134**, 685–692.
57 U. Rau, U. W. Paetzold and T. Kirchartz, *Physical Review B*, 2014, **90**, 035211.
58 C. J. Emmott, A. Urbina and J. Nelson, *Solar Energy Materials and Solar Cells*, 2012, **97**, 14–21.
59 D. Angmo and F. C. Krebs, *Journal of Applied Polymer Science*, 2013, **129**, 1–14.
60 S. De, T. M. Higgins, P. E. Lyons, E. M. Doherty, P. N. Nirmalraj, W. J. Blau, J. J. Boland and J. N. Coleman, *ACS Nano*, 2009, **3**, 1767–1774.
61 L. Yang, T. Zhang, H. Zhou, S. C. Price, B. J. Wiley and W. You, *ACS Applied Materials & Interfaces*, 2011, **3**, 4075–4084.
62 B. Azzopardi, C. J. M. Emmott, A. Urbina, F. C. Krebs, J. Mutale and J. Nelson, *Energy & Environmental Science*, 2011, **4**, 3741.
63 F. Machui, M. Hösel, N. Li, G. D. Spyropoulos, T. Ameri, R. R. Sø ndergaard, M. Jø rgensen, A. Scheel, D. Gaiser, K. Kreul, D. Lenssen, M. Legros, N. Lemaitre, M. Vilkman, M. Valimaki, S. Nordman, C. J. Brabec and F. C. Krebs, *Energy & Environmental Science*, 2014, **7**, 2792–2802.
64 B. Needles, M. Powers and S. Crosson, in *Principles of Accounting*, Cengage Learning, 11th edn., 2011, ch. 28.
65 N. Li, P. Kubis, K. Forberich, T. Ameri, F. C. Krebs and C. J. Brabec, *Solar Energy Materials and Solar Cells*, 2014, **120**, 701–708.
66 The University of Arizona Agricultural & Biosystems Engineering, *Total Areas in Major Greenhouse Production Countries*, 2012, http://ag.arizona.edu/ceac/sites/ag.arizona.edu.ceac/files/WorldGreenhouseStats.pdf.
67 N. Castilla, *Plasticulture*, 2008, **8**, 60–79.
68 J. Chang, X. Wu, A. Liu, Y. Wang, B. Xu, W. Yang, L. A. Meyerson, B. Gu, C. Peng and Y. Ge, *Ecological Economics*, 2011, **70**, 740–748.
69 Panhellenic Confederation of Unions of Agricultural Cooperatives (PASEGES), *GREENERGY: Final activity report*, September 2005, 2008.
70 M. Jørgensen, J. E. Carlé, R. R. Søndergaard, M. Lauritzen, N. A. Dagnæs-hansen, S. L. Byskov, T. R. Andersen, T. T. Larsen-olsen, A. P. L. Böttiger, B. Andreasen, L. Fu, L. Zuo, Y. Liu, E. Bundgaard, X. Zhan, H. Chen and F. C. Krebs, *Solar Energy Materials and Solar Cells*, 2013, 1–10.

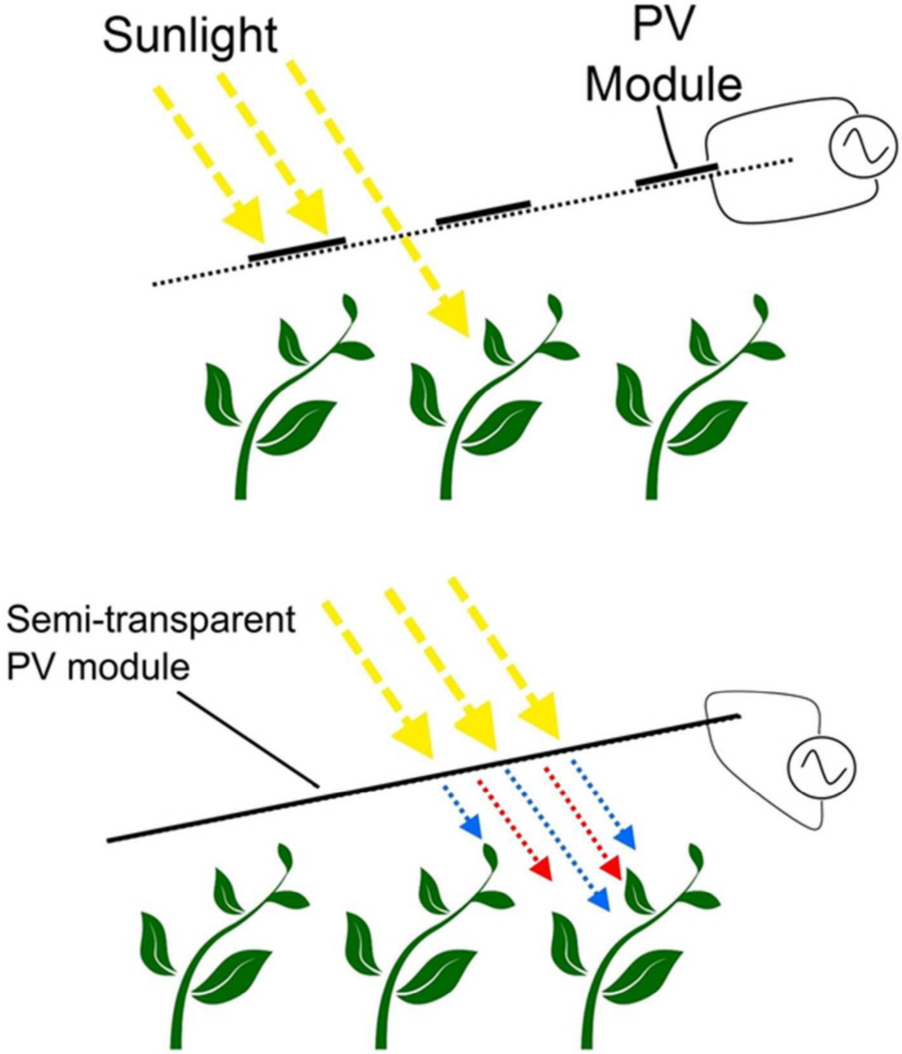

55x60mm (300 x 300 DPI)

Broader Context

Organic photovoltaics (OPV) are an emerging technology, currently being developed for large scale manufacture and with the potential to be scaled to production speeds of gigawatts per day. Yet low efficiencies of the technology may limit their deployment in certain regions due to the large land areas that would be required. However, vast areas of the world are covered in plastic, in the form of plastic greenhouses for protected agriculture. There is therefore a potential match between areas already covered in plastic and plastic photovoltaic technology, which could have a large impact in allowing further evolution in the energy system while avoiding competition for land use in agricultural areas. Although organic photovoltaics (OPV) have received huge interest in the academic literature, there has been limited analysis of the application of the technology. This study looks at an innovative use for the technology, namely the photovoltaic greenhouse and demonstrates the huge potential of this application, whilst also assessing the performance characteristics required of OPV, and how the technology compares to more mature PV technologies.